Electronic appendix

Part A

Poisson and Gamma statistics, Fourier transform and autocorrelation

We used the *Sherman's* statistics (ω_n) to assess whether the IeI distributions could be consider exponential or not (for details see Van der Kloot *et al.* 1999). In addition to a (random) Poisson renewal process, we also tested for gamma renewal processes in IeI distributions. A gamma process can be modelled by the two-parameter gamma density function $f(x \mid a,b) = t^{a-1} e^{-x/b} / \Gamma(a) b^a$, where a is the order of the gamma process, b is the characteristic time and $\Gamma(\cdot)$ is the gamma function. Independence of mIPSCs was assessed by calculating the Fourier transform of the autocorrelation function (power spectrum) of number of events per time bin (Van der Kloot *et al.* 1999).

Recurrence quantification analysis

Recurrence quantification analysis (RQA) was used to detect long-term regularities of spontaneous neurotransmitter release. RQA is a non-linear tool used to quantify the amount of deterministic structure in a data series. RQA fundamentally analyses structures in recurrence plots that can be derived from any data series. In order to obtain the plot, the time series $X(t)$, t=0,…,n-1; generates vectors with m scalar points separated in time by a delay d.

$$y(t) = \{x(t), x(d+t), x(2d+t), \ldots, x((m-1)d+t)\} \quad (1)$$

The parameter m represents the embedding dimension and the embedding matrix is given by:

$$E = \begin{bmatrix} y(0) \\ \vdots \\ y(N-1) \end{bmatrix} \quad (2)$$

$$N = n - (m-1) \quad (3)$$

The next step is to create a matrix with Euclidean distances [$d(x,y)$] between all possible vector pairs:

$$DM = \begin{bmatrix} d(E_{1,row(1)}, E_{1,row(1)}) & \cdots & d(E_{1,row(1)}, E_{N,row(N)}) \\ \vdots & \ddots & \vdots \\ d(E_{N,row(N)}, E_{1,row(1)}) & \cdots & d(E_{N,row(N)}, E_{N,row(N)}) \end{bmatrix} \quad (4)$$

The recurrence plot (RP) is then obtained by graphing points in the matrix in which the distance is equal or smaller than a radius *r* (recurrent points). The choice of values for *d*, *m* and *r* is examined further in the *Discussion*. Random processes generally generate RP's with scattered recurrent points forming no or very few segments while non-random processes can form patterns. Examples of RP's of known functions can be seen in Figure 5A (*d*=3, *m*=5 and *r*=0.5 for all plots). Patterns in these plots can be generally examined by eye. The RP is an extension of the autocorrelation function, and simple inspection can help to identify the nature of the system. Diagonal structures parallel to the main diagonal (MD - 45^o) imply that the trajectory of the signal segment is parallel to the temporal evolution and diagonal segments perpendicular to the main diagonal (135^o) represent trajectories that are contrary to the temporal evolution. In other words, diagonal segments parallel to the MD suggests that the system is similar at different times with evolution directly related to the time and perpendicular segments suggest similarity at diverse times with counter-temporal evolution (deterministic systems). The RP can also suggest chaos if diagonal segments are followed (or preceded) by isolated recurrent points. Horizontal and vertical segments indicate that the system does not vary or does so slowly. In Figure 5A we show four examples of RPs generated by different systems. A simple sinusoid produces mostly diagonal segments, the distance between similar patterns corresponding to the period (Figure 5A, top-left). If the sinusoidal period varies with time (eg. a chirp), the direction of the segments can indicate if this variance is in favour or contrary to the temporal evolution. For example, in Figure 5A, top-right, the chirp period increases with time and the diagonal segments angle moves away from 45^o. In Figure 5A, bottom, a chaotic system (Lorenz attractor – eq. 5) produces diagonal segments followed by single recurrent points and vertical/horizontal lines where the system evolution is slow (2nd quadrants of the two bottom RPs). The Lorenz attractor is derived from a simple model of weather patterns developed by the meteorologist Edward Lorenz in 1963, and it is commonly expressed by a system of three differential equations:

$$\begin{aligned} \dot{x} &= a(y - x) \\ \dot{y} &= x(b - z) - y \\ \dot{z} &= xy - cz \end{aligned} \qquad (5)$$

where *a*, *b* and *c* are constants. The series, an example of deterministic chaos, does not form limited periods nor reach a steady state and is sensitive to initial conditions.

Statistical assessment of geometrical structures in RP is necessary when patterns are difficult to distinguish. Hence, recurrence quantification extracts variables that can be used for the recurrence plot analysis: %recurrence, %determinism, *maxLine*, entropy, %laminarity (*%lam*) and trapping time (*TT*). %recurrence is the percentage of the plot occupied by recurrent points. If the RP is contained in the matrix $R_{i,j}$, the recurrence ratio (*rec*) is equal to $rec = \frac{1}{N^2}\sum_{i,j=1}^{N} R_{i,j}$. %determinism is the number of recurrent points

that form diagonal structures (line segments of at least 2 points). In other words, it distinguishes between points that are individually dispersed and those that are organized into specific diagonal patterns. If the distribution frequency of diagonal lines with length l in the RP is equal to $P(l) = \{l_i; i = 1...N_l\}$, where N_l is the number of diagonal segments, the determinism ratio (*det*) is defined by:

$$Det = \frac{\sum_{l=2}^{N} l * P(l)}{\sum_{i,j}^{N} R_{i,j}} \qquad (6)$$

maxLine is the maximum length of diagonal segments. Entropy estimates the 'richness' of deterministic structures in the series and is calculated from distributions of lengths of diagonal lines parallel to the MD using principles of Shannon's information theory. It is defined by $entropy = \sum_{l=l_{\min}}^{N} p(l)\ln[p(l)]$ with $p(l) = P(l) \Big/ \sum_{l=2}^{N} P(l)$. Usually, the probability for line segments with similar lengths decreases as a function of length. Periodic systems generally have high entropy (diversity of diagonal segments) while chaotic systems have low entropy (few diagonal segments). While %determinism and %recurrence characterise recurrence plots according diagonal structures, vertical lines also provide useful information about the nature of the system. Analogous to %determinism, %laminarity (%*lam*) computes the percentage of points in the recurrent pots forming vertical structures:

$$\%lam = \sum_{k=k_{\min}}^{N} k.P(k) \Big/ \sum_{k=1}^{N} k.P(k) \qquad (7)$$

where k are vertical structure lengths and $P(k)$ is the distribution of vertical lines in the recurrence plot. The mean length of vertical structures (trapping time – *TT*) is also calculated: $TT = \sum_{k=k_{\min}}^{N} k.P(k) \Big/ \sum_{k=k_{\min}}^{N} P(k)$, and it measures the mean time (or number of samples) in which the system changes states. Further details in RQA can be found in Marwan *et al.* (2002). A powerful RQA Matlab © (Mathworks, USA) toolbox was used to compute some of the RQA calculations in this manuscript. This toolbox is freely available at 'http://www.agnld.uni-potsdam.de/~marwan/toolbox/'. We have also used custom made Matlab © routines to perform early RQA computations.

Lyapunov exponent

In order to test if the dynamics of mIPSCs are chaotic we calculated the maximal Lyapunov exponent of the mIPSC IeI. Lyapunov exponents are a measure of the rate at which orbits on an attractor converge or diverge as the system evolves in time (Rosenstein *et al.* 1993), and provide a direct measure of the stability of those orbits. The largest Lyapunov exponent (lLe) calculates the maximum average rate of divergence. If the lLe is positive, it indicates global instability and sensitivity to initial conditions, which defines the presence of chaos. A full detailed explanation in the Lyapunov exponent calculation can be found in Rosenstein *et al.* (1993).

Allan Factor

The Allan factor ($A(T)$) is obtained by dividing the Allan variance by twice the average of the event count. The Allan variance is defined by the mean variation in the difference of adjacent counts. In order to calculate the $A(T)$, mIPSC recording times of total length L are partitioned into windows with duration T. With $Z_k(T)$ equal to the number of mIPSCs in each window, the $A(T)$ is then given by:

$$A(T) = \frac{\sum \left[Z_{k+1}(T) - Z_k(T) \right]^2}{2 \sum Z_k(T)} \qquad (8)$$

If event clusters at a certain scale are present in the data, $A(T)$ will rise at this particular time scale. However, if the data displays fractal behaviour, one will observe hierarchies of clusters of different durations, causing the $A(T)$ to continuously rise as each cluster time scale is incorporated in turn (the logarithmic plot $A(T)$ versus T will be a straight line). Surrogate data obtained by shuffling the data series can be used to compare original $A(T)$ to datasets where fractals were disrupted. If the power law relationship between $A(T)$ versus T is a positive slope α in the loglog scale the data might display fractality. We used the correlation coefficient (r) to test for linearity in logarithmic $A(T)$ vs. T plots. When $0 < \alpha < 1$, the Hurst exponent (H) can be calculated by $H = (\alpha + 1)/2$. H tests for the presence and degree of long-range dependency (Fadel *et al.* 2004). The H is a measure of self-similarity (fractals) and long-term memory in Gaussian processes. In general terms, if H=0.5, the data series is similar to a random walk, while $0.5<H<1$ indicates 'persistent' behaviour (positive autocorrelation) and $0<H<0.5$ suggests 'anti-persistent' behaviour (i.e. long IEI's is followed by short ones).

Classification of mIPSC IeI data

In Figure 5B we summarise the decision tree we used to classify our mIPSC IeI data. The inspection of RP can lead to the next available non-linear (or linear) tool to classify whether the data is periodic, self-similar, chaotic or random. In case of evident periods, the Fourier transform can estimate the frequency (or frequencies) of the periodic component and CWT could describe the evolution of the frequency

components in time. In case of self-similarity, further tests for fractals are required and if a memory process is detected, the system can be reassessed for self-similarities using CWT. If RP's are suggestive of chaos, the maximal Lyapunov exponent is calculated and it's value can be correlated to 1/*maxLine* to verify if the exponent calculation is not erroneous due to embedding and/or dataset length problems.

Choosing parameters for RQA

RQA is greatly dependent on the chosen delay (*d*), dimension (*m*) and radius (*r*). There is no appropriate context for an ideal *d* (Zbilut *et al.* 2000). The delay has to be large enough to contain only relevant dynamics, ignoring the noise. In this study we empirically fixed the *d* equals to 3 for all datasets. The dimension was also chosen to be the same (m=5) for all data sets. A theoretical approach to the size of *m* is given in Filligoi and Felici (1999). According to these authors, dimension should satisfy the topological relationship $m = 2v + 1$ (where *v* is the number of variables interacting with the system). However, it was impractical to determine *v* in this study. We therefore carried out the analysis using various dimensions and the value of 5 was chosen as it was the first value for *d* which RQA variables became asymptotic. The value for *r* (r=0.5) was obtained by assessing the modelled mIPSC's, fixing r=0.5 showed sensitivity to the presence of the periodic component within the random series without 'false-positives' or 'false-negatives'. Evaluating chaos or fractality in small datasets is a problematic issue. RQA can detect chaotic behaviour using relatively few points. Some RQA applications can detect changes in system complexity using less than 100 samples (Marwan *et al.* 2002). Therefore, the use of RQA can complement and amend the calculation of Lyapunov exponents. Moreover, 1/*maxline* is directly correlated with the maximal Lyapunov exponent (Marwan 2003). According to the original work, the method used here could accurately compute the maximal Lyapunov exponent in a data series with *N*'s as little as N=100 and undergoes little influence from a different embedding dimension or delay (Rosenstein *et al.* 1993).

Part A, Acknowledgments

We thank Dr. N. Marwan and collaborators for making the CRP toolbox freely available.

Part A, References

Marwan, N. 2003 Encounters with neighbors: current developments of concepts based on recurrence plots and their applications. PhD Thesis, Universität Potsdam.

Filligoi G & Felici F. 1999 Detection of hidden rhythms in surface EMG signals with a non-linear time-series tool. Med Eng Phys 21(6-7):439-48.

Marwan, N., Wessel, N., Meyerfeldt, U., Schirdewan, A. & Kurths, J. 2002 Recurrence Plot Based Measures of Complexity and its Application to Heart Rate Variability Data, Physical Review E. 66(2): 026702.

Rosenstein, M.T., Collins, J.J. & De Luca, C.J. 1993 A practical method for calculating largest Lyapunov exponents from small data sets. Physica D. 65:117-134.

Van der Kloot, W., Andricioaei, I. & Balezina, O.P. 1999 Examining the timing of miniature endplate potential releases at the frog and mouse neuromuscular junctions for deviations from Poisson Expectations. Pflugers Arch – Eur J Physiol. 438: 578-586.

Zbilut JP, Thomasson N, Webber CL. 2000 Recurrence quantification analysis as a tool for nonlinear exploration of nonstationary cardiac signals. Med Eng Phys. 24(1):52-60.

Part A, Figure 5. Recurrence plots of periodic and chaotic functions. A. RP's of various functions. The underlying data series is represented over the top of each RP box. *Top-left,* RP of a sinusoid; *top-right*, RP of a chirp; *bottom-left* and *right*, RP produced by the *x* and *z* coordinate of a Lorenz attractor respectively (see text for details). B. General algorithm for the classification of mIPSC IeI. RP indicates if intervals are periodic, chaotic and/or fractal. Further analysis using fast Fourier transform (FFT), wavelet transform (WT), Lyapunov exponents (Lyap), Allan factors ($A(T)$) and Hurst exponent (H).

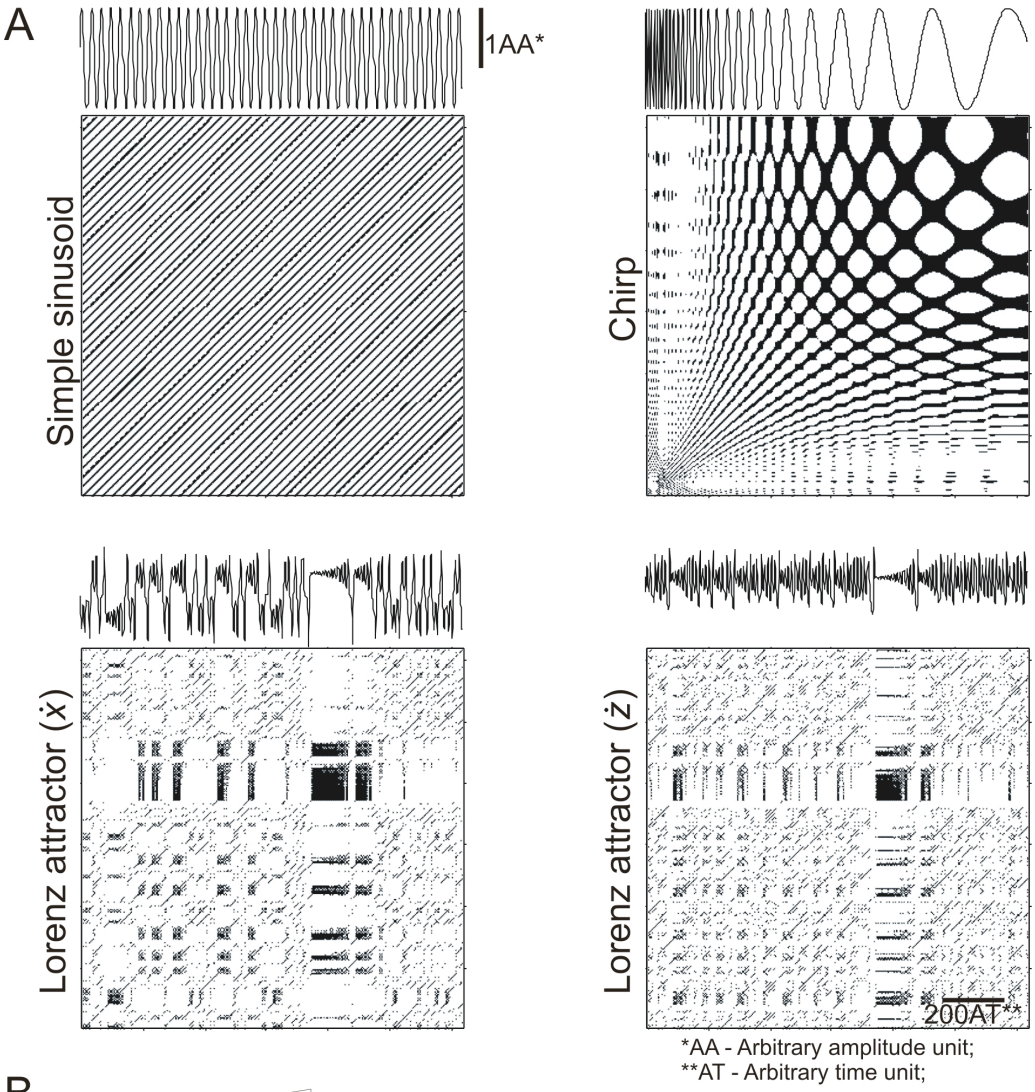

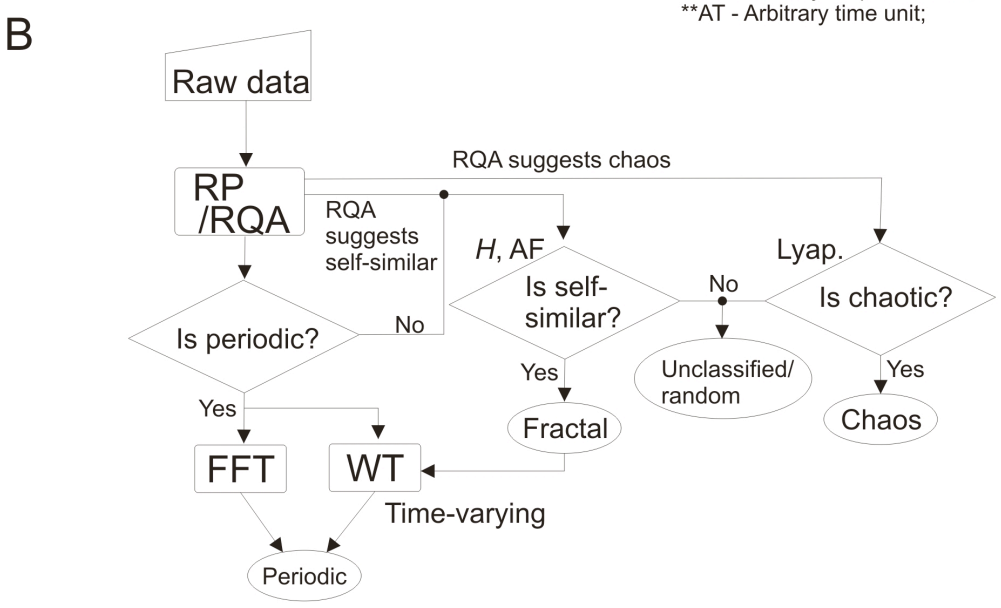

Part A, Figure 5

Part B

Table 1. Effect of thapsgargin in RQA

RQA variable	Control	Thapsgargin
%recurrence	31±6%	3±1%*
%determinism	21±5%	0.6±0.02%
maxLine	23±3.4s	11s**
Entropy	1.24±0.1	1.2±0.21
%lam	37±6%	4±0.7%
TT	5.6±0.4s	4.3±0.3s

*p<0.05; **Only possible to estimate in 1 cell

Part C

Continuous Wavelet Transform

In case of negative α's in $A(T)$ vs. T loglog plots (suggestive of periodicity), a continuous wavelet transform (CWT) was used in order to assess periodic components of the signal in time. The temporal resolution of the frequency estimation is adequate to follow frequency transients of the signal in the time domain. (Leao & Burne 2004). The continuous WT of a signal *x(t)* is defined as $CWT_x(a,b) = \int x(t)\psi^*_{a,b}(t)dt$ (with $a \neq 0$). The basis function results from the scaling of the mother wavelet ψ at time *b* and scale *a.* By increasing or decreasing *a*, the basis function is fitted to a segment of *x(t)*; hence, *a* indirectly represents frequency components of the signal. We used the first derivative of the Gaussian function ('*sombrero*' function) as the mother wavelet (Daubechies 1994). We chose the *sombrero* function as the mother wavelet as this function is real and it gave a good reconstruction of the transformed signal. The plot formed by *a* vs. *b* is called scalogram and it can also display self-similarities of the signal in the time-frequency plane. For details in CWT calculations see Leao and Burne (2004). IeI's from 2 normal mice control cells with $\alpha > 0$ (example in Figure 5A – cell 1) were also analysed using CWT (Figure 5B). Despite the power spectrum being flat, when local maxima values of *a* are plotted against time slow oscillations are revealed (cell 1, 0.04Hz and cell 5, 0.03Hz). RQA, $A(T)$ (α and r) and Lyapunov exponent values of the two cells showed in Figure 6 are summarised in Table 2.

Part C, References

Daubechies, I. 1994 Ten lectures on wavelets. *CBMS, SIAM*; 61:194-202.

Leao, R.N. & Burne, J.A. 2004 Continuous wavelet transform in the evaluation of stretch reflex responses from surface EMG. J Neurosci Methods 133(1-2):115-25.

Part C, Figure 6. Periodic and aperiodic spontaneous neurotransmitter release. A, B, C and D left panels are related to cell 1 (case 1 – periodic mIPSC's) and right panels to cell 12 (case 2 – aperiodic mIPSC's), both from normal mice under control conditions. Scale bars in (A) and (B) represent 200 IeI's. A. IeI and their respective RP's. B. Scalograms of the IeI's in (A). C. Spectrograms of the events in (A). D. Local maxima of the scalograms in (B) plotted against mIPSC time.

Part C, Table 2. Nonlinear assessment of a cell with periodic and non-periodic mIPSCs

	C1 (periodic)	**C12 (aperiodic)**
%recurrence	16.2%	9.6%
%determinism	4.9%	2%
maxLine	26s	13s
Entropy	1.69	1.13
%lam	12.6%	8.5%
TT	3.7s	4s
Max. Lyapunov	1.6	2.04
A(T) - *(α , r)*	-0.02, -0.62	0.03, 0.71

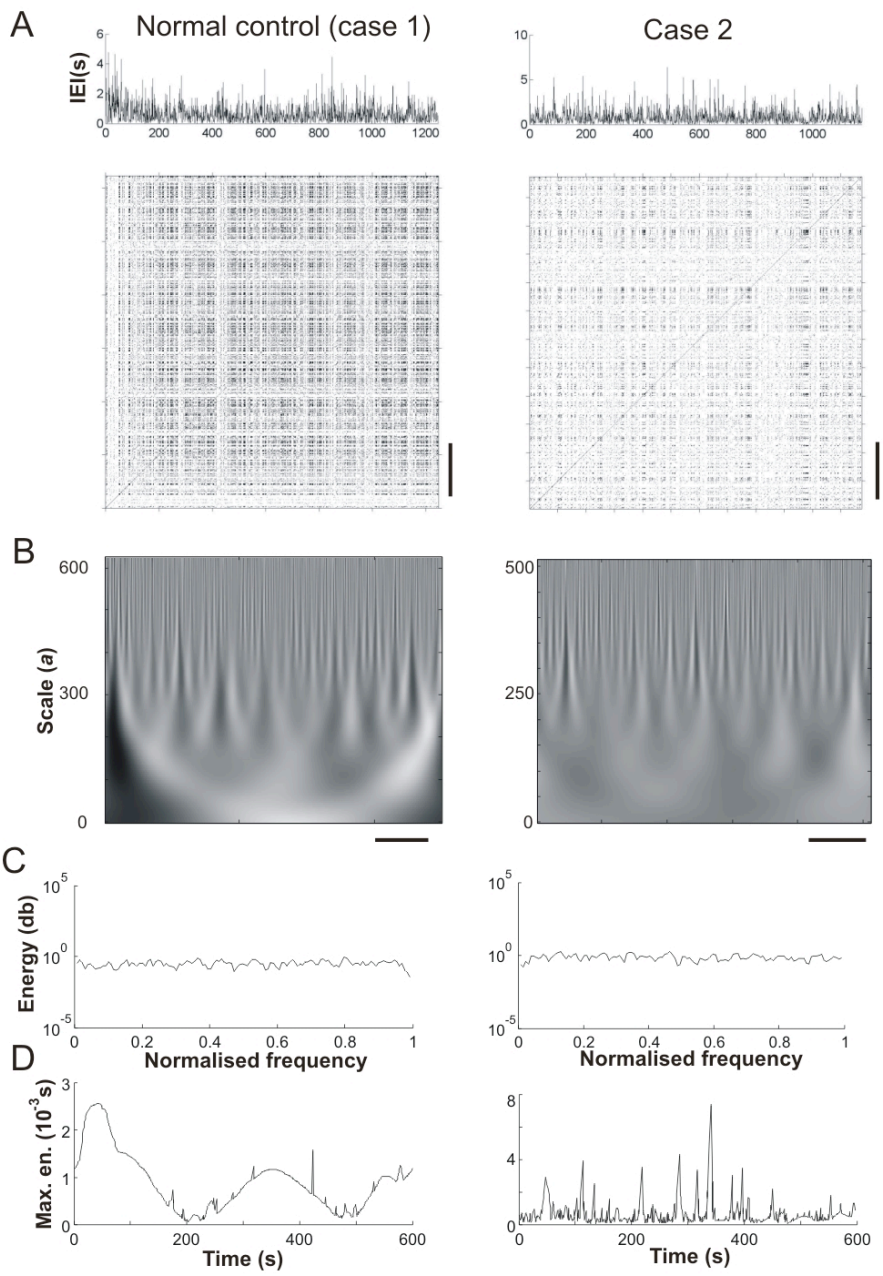

Part C, Figure 6